ENGINEERING ASPECTS ON FATIGUE CRACK GROWTH UNDER COMPLEX LOADING

F. Nilsson, M. Olsson and B. Alfredsson
KTH, Department of Solid Mechanics
SE-100 44 Stockholm, Sweden

ABSTRACT
Fatigue crack growth experiments were performed for different types of complex loading involving variable amplitude loading, mixed mode loading and contact loading. The growth processes were analysed by combinations of engineering and numerical methods.

1. INTRODUCTION

In spite of significant advances during the last decades fatigue crack growth is still a challenging problem. When the loading situation is complex the methods for prediction are far from fully developed. Even for those cases when the mechanisms are known to some degree, there remains to develop engineering methods so that the techniques can be used for assessment of practical cases.

2. VARIABLE AMPLITUDE MODE I CRACK GROWTH

Mode I growth under variable amplitude loading provides one example of load complication. There is now general agreement that if the crack closure effect can be properly accounted for then quite accurate predictions can be made. To predict crack closure under variable conditions by full finite element simulation is far from easy. In the present work we employed an engineering type of technique to provide approximate estimates for the growth rate under block loading based solely on experimental data. It is assumed that the crack growth can be described by eqn (1).

$$\mathrm{d}a/\mathrm{d}N = \dot{a}_0\left(\Delta K_{\mathrm{I}}^{\mathrm{eff}}/K_0\right)^{\beta_{\mathrm{eff}}}. \tag{1}$$

The material constants K_0 and β were determined by using a so-called constant K_{Imax} testing strategy. Variable amplitude experiments on the material AISI 101 were performed using Compact Tension (W=50 mm) specimens for block loading according to Fig. 1. The large cycles had R=0.05 and $\Delta K_{\mathrm{I}}^{\mathrm{nom}}$ = 40 $\mathrm{MP}\sqrt{\mathrm{m}}$ in all experiments while the small cycles had different values of $\Delta K_{\mathrm{I}}^{\mathrm{nom}}$ and R according to Table 1. For analysis of the block loading case it was assumed that the closure level was determined by the large cycles and maintained during the process. It was further assumed that the closure level was the same as for constant amplitude tests with a corresponding R-ratio, Describing the crack growth in terms of nominal $\Delta K_{\mathrm{I}}^{\mathrm{nom}}$ by an equation of the type (1) leads to R-dependent constants $K_0(R)$ and $\beta(R)$. By using the definitions of nominal and effective ranges the closure level can be obtained from eqn (2).

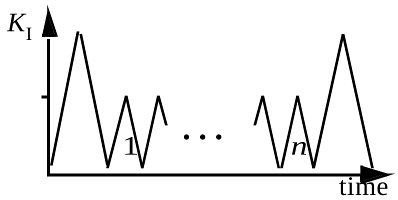

Fig. 1. Load blocks, n = number of small cycles.

$$K_{\mathrm{I,cl}} = K_{\mathrm{I,max}} - K_0^{\mathrm{eff}} \left(\Delta K_{\mathrm{I}}^{\mathrm{nom}} \big/ K_0(R) \right)^{\beta((R)/\beta_{\mathrm{eff}}} . \tag{2}$$

The results from the different experiments are displayed in Table 1 and the agreement between measured and predicted rates was remarkable. Further details can be found in Månsson *et al.* [1] and the same method applied to surface cracks growth in Nilsson *et al.* [2].

Table 1. Comparison of measured and predicted mean growth rates.

n	$\frac{K_{\mathrm{I}}^{\mathrm{small}}}{\mathrm{MPa}\sqrt{\mathrm{m}}}$	R_{small}	Predicted mean growth rate/ $\mathrm{nm} \cdot \mathrm{cycle}^{-1}$	Measured mean growth rate/ $\mathrm{nm} \cdot \mathrm{cycle}^{-1}$
1	20	0.095	188	184
10	20	0.095	57	66
10	20	0.38	80	80
10	20	0.38	80	78
10	12	0.5	41	40
10	12	0.5	41	40
32	8.7	0.175	8	10
32	16.6	0.1	21	21
32	21.2	0.08	43	40

3. MIXED MODE LOADING CRACK GROWTH

Fatigue loading on a cracked structure will subject the crack front to time dependent mixed mode loading. The most general loading will include continuous variation of load magnitude, direction and point of application. Here, we consider a situation where 1) one loading type is dominating (in terms of numbers of applications) and 2) distinct cycles can be identified, acting in sequence. Then, the crack path will adjust itself so that the dominating load type gives a pure mode I state at the crack front. In order to find practical guidelines for this situation, an experimental series has been conducted. In the tests, a fatigue crack is propagated in pure mode I, a single mode II load is applied. Thereafter, the mode I fatigue loading is continued. In the literature, diverging result have been reported for the crack growth rate during the mode I loading following after the mode II load.

The material was a work tool steel of high and uniform quality AISI 01, with Young's modulus E = 208 GPa, yield strength σ_{Y} = 440 MPa, Poisson's ratio ν = 0.3 and closure free Paris law data C = 0.00468 and n = 3.13 (ΔK in $\mathrm{MPa}\sqrt{\mathrm{m}}$ and da/dN in nm/cycle). The average grain size was approximately 16 μm. The specimens were of CTS type, with width W = 70 mm, thickness t = 10.65 mm and distance from loading holes to crack plane c = 50 mm. Initial crack length was 20 mm, mode II loading was performed at 27 mm, and final crack length was 60 mm. Four tests were performed, with K_{II} = 0, 20, 30 and 40 $\mathrm{MPa}\sqrt{\mathrm{m}}$, respectively. The mode I loading was always ΔK_{I} = 20 $\mathrm{MPa}\sqrt{\mathrm{m}}$, R = 0.1. The pure mode I test (with zero mode II loading) was a reference test. It is known that da/dN will vary slightly with crack length even for constant ΔK_{I}. This variation was expressed with a second order polynomial. The results for the three remaining tests are presented as crack growth rate subtracted with the reference test growth rate, i.e. da/dN - (da/dN)$_{\mathrm{ref}}$. In this way, the deviation from the mode I growth for the test with K_{II}=0 was clarified.

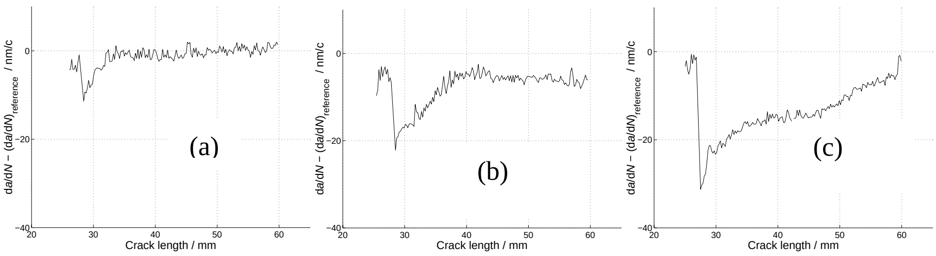

Fig 2. The change in growth rate in mode I due to a single mode II load of 20, 30 and 40 MPa $\sqrt{\text{m}}$ in (a), (b) and (c) respectively.

A dip in growth rate after the mode II load is visible; thereafter the crack growth rate slowly increases. The distance it takes to reach the original mode I value is a recovery distance, RD. In the three tests, we found RD = 6, 12 and 32 mm, respectively. The reason for the reduction in crack growth rate was permanent relative tangential displacement of crack surface irregularities. This increase the closure level and crack growth rate is strongly connected to the effective stress intensity factor range, $\Delta K_{\text{I, eff}}$. A naïve consideration of the influence from a single mode II load would be that it has no influence at all, or even that it increases the growth rate. Here, we see that the rate was substantially reduced. It is emphasized that the effect was dominated by crack closure. This means that for mode I loading at high *R*-value the growth rate reducing effect of mode II loading is not present at all. Further details on the experiments can be found in Dahlin and Olsson [3].

4. FATIGUE CRACK PATHS DURING COMPLEX LOADING

The prediction of a fatigue crack path is far from obvious when the stress state is multi-axial and the relations between stress components develop non-proportionally during the load cycle. In such cases the fatigue crack propagates through a stress field with different stress gradients for the different stress components in both space and during the load cycle.

An example of this stress state is in the neighbourhood of cyclically loaded contacts. Three such situations have been investigated. In the first series a spherical indenter was repeatedly pressed against a flat test specimen either with pure normal or inclined loads, see Alfredsson and Olsson [4]. The second and third series comprised of fretting experiments, again with spherical indenters, see Cadario and Alfredsson [5]. In the second series, the bulk and the normal contact loads were both constant during each experiment. The fretting load was applied as a cyclic tangential contact load directed in the same direction as the bulk load. The third experiment was a traditional fretting test with in-phase cyclic bulk and tangential contact loads.

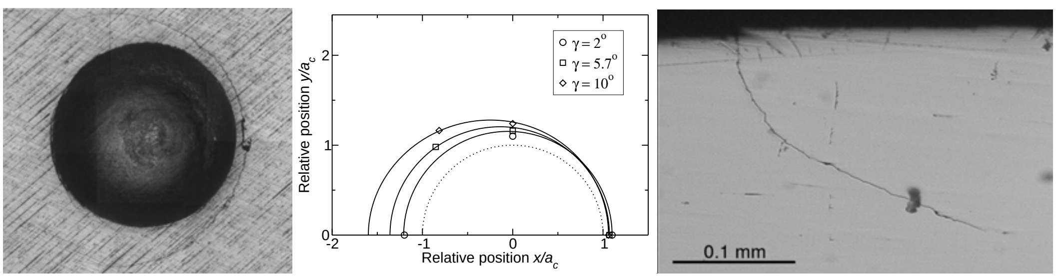

Fig 3. (a) Contact mark with elliptically shaped surface crack from a 10° inclined load. (b) Crack path in surface compared to numerical solution. (c) Cross-sectional view of fatigue crack from purely normal contact load.

After all experiments, circular contact marks remained in the contact surface together with one or two large fatigue cracks that had developed from the contact surface and grown into the test specimen material. Due to differences in load history the position for crack initiation and the subsequent crack growth differed between the series. In the cases with cyclic but pure normal or inclined contact loads, *i.e.* in-phase normal and tangential loads, the fatigue crack started at the surface but a short distance outside the contact mark. In the surface view the crack grew around the contact mark whereas in the cross-sectional view it propagated in the outward direction. With increasing inclination angle, or increasing tangential load, the surface-growing crack receded from the contact following an elliptic path (Fig. 3a). In the cross-sectional view the outward angle defined from the surface to the extended crack increased with increasing tangential load (Fig. 3c). For both types of fretting experiments, on the other hand, the cracks started inside the contact zone, in the area close to the contact rim where micro-slip existed during cyclic loading. If only the tangential load was cyclic, then the crack followed an ellipsoidal shape below the contact where it halted (Fig. 5a). For fretting tests with in-phase cyclic bulk and tangential loads the crack first grew toward the interior of the contact but then they turned to a direction normal to the bulk load and grew through the specimen (Fig. 6a).

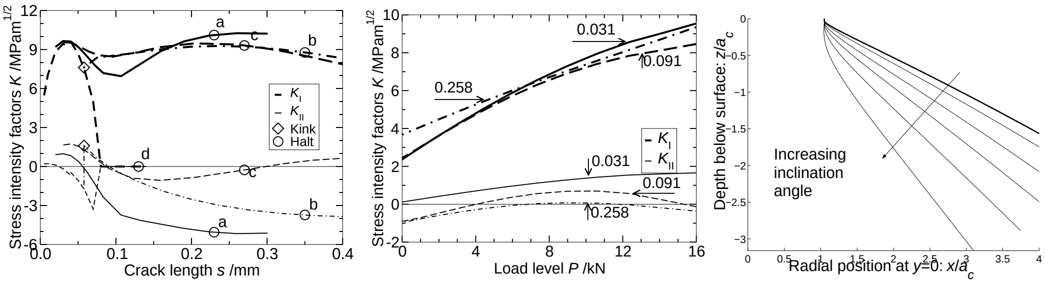

Fig 4. Mode I and II loads from normal contact (a) along some crack paths; (b) at some crack tip positions during a load cycle. (c) Simulation of crack path in cross-section for inclined contacts.

The mode I and II stress intensity factors were computed along the cross-sectional crack paths for some fatigue cracks that resulted from purely normal contact load (axial-symmetric case). Although the individual crack results exhibited deviations, the cracks turned during propagation to reduce the mode II load on the crack tip, *i.e.* the cracks turned to follow a path with the maximum mode I load (Fig. 4a). Since stresses were non-proportional, the mode II crack tip load ranged from positive to negative values during the load cycles giving non-zero ΔK_{II} (Fig. 4b). Furthermore, ΔK_I and K_{Imax} were almost equal in this case.

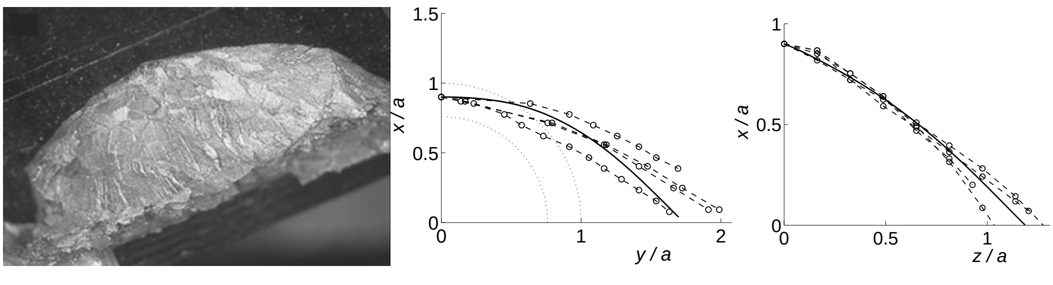

Fig 5. Fretting crack at constant bulk load. (a) Ellipsoidal crack. (b) Surface view and (c) cross-sectional view of experimental and simulated crack paths.

The process of computing mode I and II stress intensity factors along a crack path is time consuming, particularly when the loads and crack geometry are such that a FE-analysis, including the contact, becomes fully three-dimensional. This situation exists for the inclined contact load and both fretting cases. An approximate method to predict the crack paths was therefore tested, utilizing three assumptions. Firstly, it was assumed that the crack follows the direction of the largest mode I SIF range. Secondly, the mode I SIF range was assumed to follow the direction of the largest principal stress range. Thirdly, during a non-proportional stress cycle the direction of the largest principal stress range rotates. Therefore, a stress range tensor, $\Delta\sigma_{ij}$, was computed with the range of each individual stress component. The largest principal stress direction for this range tensor was finally used to simulate the crack paths (Figs 3b, 4c, 5b, 5c, 6b and 6c).

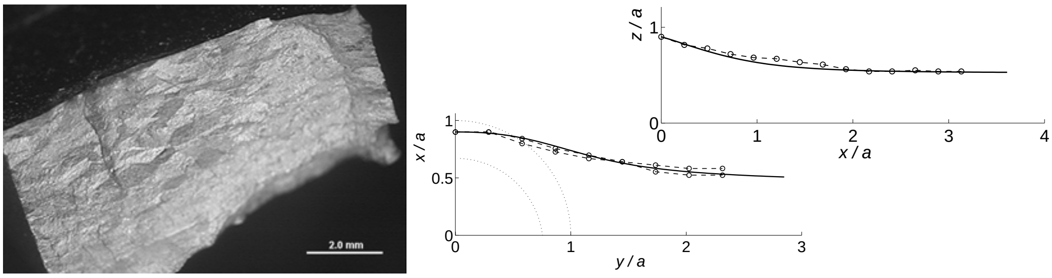

Fig 6. Fretting crack at cyclic bulk load. (a) Almost straight crack. (b) Surface and (c) cross-sectional views of experimental and simulated crack paths.

References

1. Månsson, T. Öberg, H. and Nilsson, F., *Engng Fracture Mech.*, 2004, Vol. 71, 1273-1288.
2. F. Nilsson, T. Hansson and T. Månsson, *Engng Fracture Mech*, Vol. 71, 2004, 1725-1735.
3. Dahlin, P. and Olsson, M. *Int. J. Fatigue*, 2004, in press.
4. Alfredsson, B. and Olsson, M., *Fat. Fract. Engng Mater. Struct.*, 2003, **26**, 589–602.
5. Cadario, A. and Alfredsson, B. *Engng Fracture Mech*. Submitted for publication.